Production of nanopowders of bismuth oxide doped with silver by pulsed electron beam evaporation in vacuum

Production of nanopowders of bismuth oxide doped with silver by pulsed electron beam evaporation in vacuum

V G Ilves[1], S Y Sokovnin[1,2] and M A Uimin[2,3]

[1] Institute of Electrophysics, 106 Amundsena St., Yekaterinburg, 620016, Russia
[2] Ural Federal University, 19 Mira St., Yekaterinburg, 620002, Russia
[3] M N Mikheev Institute of Metal Physics, 18 S. Kovalevskaya St., Yekaterinburg, 620108, Russia

E-mai: ilves@iep.uran.ru

Abstract. Various bismuth containing compounds are promising in many applications, including for creating photocatalysts based on them using a visible range of light. However, strong polymorphism (9 polymophic phases of Bi_2O_3), thermal instability and changes in the properties of bismuth oxide during long-term storage significantly complicate work with it. One way to increase stability and improve photocatalytic properties is by doping Bi_2O_3 with various metals. Ag doped Bi_2O_3 nanoparticles (NPs) are typically produced using chemical techniques often associated with the presence of toxic chemicals. The present paper used an environmentally friendly method of producing NPs using the method of pulsed electron beam evaporation in vacuum. The evaporation target was obtained by solid phase synthesis in an electric furnace on air using silver nitrate additives (1 and 5 wt.%).Textural, thermal and magnetic properties of the obtained NPs have been studied. Was found that the Ag-Bi_2O_3 NPs have a specific surface area (SSA) of 23.7 m^2/g, which was almost 2 times bigger than the SSA of the pure Bi_2O_3 (13.2 m^2/g) obtained previously. The thermal stability of the Ag-doped Bi_2O_3 samples was maintained to the temperature 350°C. While further heating on air took place the phase transition $\beta \rightarrow \alpha$.

1. Introduction

Nanoparticles (NPles) Bi_2O_3 are attractive for use as photocatalysts [1]. Of the nine polymorphic forms of Bi_2O_3 [2], β-phase Bi_2O_3 [3] has the greatest photocatalytic activity, but it is characterized by low thermal stability. Doping Bi_2O_3 by various elements is one of the ways to increase the thermal stability and photocatalytic activity of β-phase [4]. The purpose of the present work was to study the effect of silver content on the formation and stability of β-phase Bi_2O_3 using the pulsed electron beam (PEBE) evaporation method in vacuum [5].

2. Experimental section

2.1. Materials

Oxide bismuth (III) micron powder (Bi_2O_3), analytic grade, GOST 10216-80 and nitrate silver ($AgNO_3$) of CP grade, GOST 1277-75 were used to produce Ag doped-Bi_2O_3 NPles.

2.2. Synthesis of Ag doped Bi_2O_3 nanopowders (NPs) in vacuum

The evaporation targets were prepared according to the following procedure: $AgNO_3$ crystals were previously ground in a porcelain mortar and then mixed with micron powder Bi_2O_3 in mass ratios- Bi_2O_3: $AgNO_3$ = 99:1 and 95:5. Compacts were made from mechanical mixtures of powders, which were then annealed at a temperature of 500°C in air for 30 minutes (decomposition temperature $AgNO_3$ is 350°C). Further, the compacts were re-crushed in a mortar to distribute silver more evenly in the mixtures. From annealed mixtures, targets were made on a manual press, in a titanium mold. The diameter of the targets was 40 mm, height up to 1-1.5 mm, weight about 60 g. The targets were annealed in air at a temperature of 500-600°C for 30 minutes and cooled together with the furnace to room temperature. The evaporation mode of the targets: accelerating voltage – 38 kV, beam current – 0.3 A, pulse duration – 100 μs, repetition rate – 100 Hz, evaporation time – 45 minutes, beam scanning on the surface of the target – 12 cm^2, the amount of evaporated material was – 4.4 g, NPs collection (excluding losses) – 3.1 g (72.3%). Deposition of NPles was carried out on conventional window glasses placed at a distance of 10-15 cm relative to the center of the target. The NPs were collected using a titanium foil scraper. The resulting NPs had very little adhesion to glass substrates and metal surfaces.

2.3. Characterization

X-ray structural studies were carried out at the collective use center of the Institute of Metal Physics UB RAS using a high-resolution X-ray diffractometer "Empyrean" in copper filtered radiation. Nitrogen adsorption and desorption isotherms at 77 K were obtained using Micromeritics TriStar 3000 V6.03 A. Thermal analysis of the samples was carried out on synchronous thermoanalytic complex NETZSCH STA-409. Magnetic measurements were carried out using a Faraday balance at a RT.

3. Results and discussion

3.1. Synthesis of Ag-doped Bi_2O_3 NPs

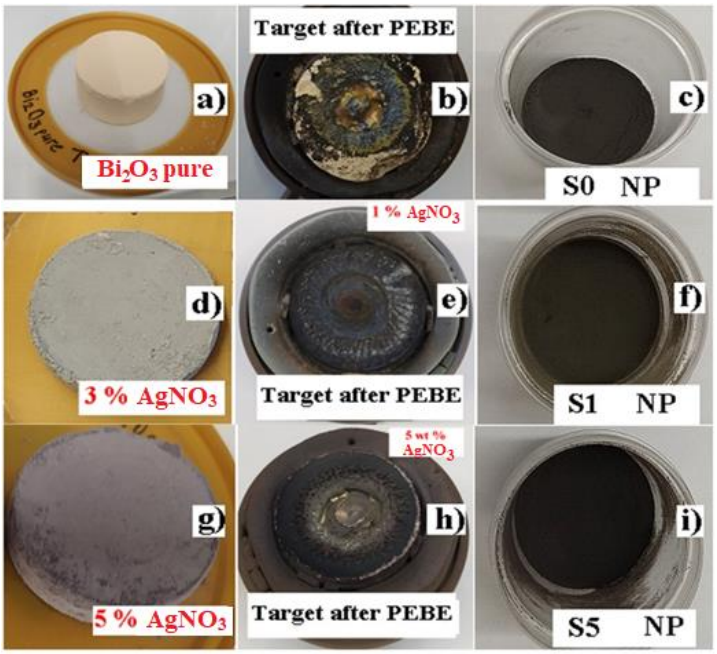

Figure 1. The target species of pure and Ag-doped Bi_2O_3 before (a, d, g) and after (b, e, h) and the corresponding NPs (c, f, i) produced by the PEBE method in vacuum collected in plastic cups.

The transformation of micron targets from pure and silver-doped powders into corresponding NPs is shown in figure 1. The characteristic metallic gloss from silver on the surface of the craters of doped

targets (figures 1 (b, e, h)) indicates the reduction of metallic Ag in vacuum and its diffusion to the surface, which is characteristic of this evaporation method.

3.2. Structural analysis and morphology of synthesized Ag doped Bi_2O_3 NPs

3.2.1. XRD analysis. Two crystal phases α- and β-Bi_2O_3, in a ratio of 16:84 wt.% and an amorphous phase (about 50-60% of the volume) [6] were found in the undoped NPs of β-Bi_2O_3 by the method X-ray diffraction (XRD) analysis. X-ray diffractograms of samples S1 and S5 are shown in figure 2. Ag-doped Bi_2O_3 NPs also contained three phases. The main crystal phase is the metastable β-phase Bi_2O_3 with a tetragonal lattice, the structure of the type Bi_2O_3 Sillenite (space group P-4b2) [7]. In figure 2 it can be clearly seen that the X-ray diffraction patterns of samples S1 and S5 contain a wide, amorphous peak near the angle $2\theta \sim 29.30°$. The content of the amorphous fraction in the samples did not exceed 10-15% of the volume of the sample. Also, a weak peak (shown by arrow in figure 2) from an unknown phase was present in both samples. As the silver concentration in the samples increased, the intensity of this peak increased, which could indicate the presence of Ag in an unspecified phase. However, we were not able to find in our X-ray bases a compound with Ag, Bi and/or O having such reflection. The mean size of coherent scattering regions (CSR) in samples S1 and S5 increased to 22 and 25 nm, respectively, compared with the CSR of sample S0 equal to 8-10 nm [6].

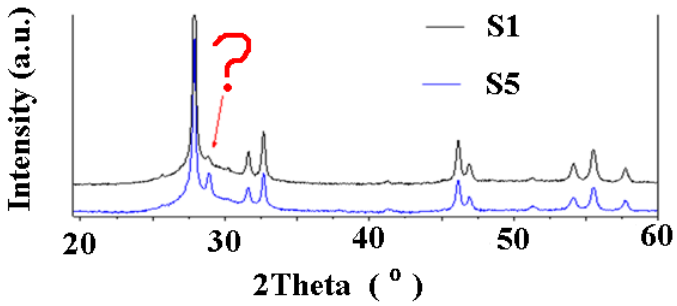

Figure 2. X-ray diffraction pattern of Ag-doped NPs prepared in vacuum: (a) S1; (b) S5.

3.2.2. Textural analysis. Figure 3 shows isotherms of adsorption-desorption of powders Bi_2O_3 pure (micro and nano sizes) and Ag-doped Bi_2O_3 (1 and 5% $AgNO_3$) of NPs and their pore size distribution relationships. To establish the possible effect of the specific surface area (SSA) of Ag doped Bi_2O_3 NPs on their physicochemical properties, we tested samples of NPs and target (table 1). The micron powder (S_{target}) had a SSA of 1.4 m^2/g. The nitrogen isotherms of samples S0 and S_{target} in (figure 3 (a, c)) belong to the IV type with an H3 hysteresis loop according to UIPAC classification. SSA NPs increased by more than 9 times compared to SSA of the starting powder, pore volume increased by almost 3 times. Doping of Ag resulted in a nearly 2-fold.

Table 1. Results BJH analysis.

Samples	SSA (m^2/g)	Pore size (nm)	Pore volume (cm^3/g)
S_{target}	1.4	36.2	-
S0	13.2	32.5	0.11
S1	20.3	24.2	0.15
S5	23.0	23.6	0.10

At a low concentration of Ag, the pore volume grew 1.5 times, then returned to the original value at a higher concentration of Ag. The radius of the Ag^+ ion (0.115 nm) slightly exceeds the radius of the Bi^{3+} ion (0.103 nm), which contributes to the formation of a solid solution of Ag in the lattice Bi_2O_3. Nevertheless, emergence of additional peak on X-ray diffractogram of Ag-doped Bi_2O_3 indicates the need to reduce the amount of additive-$AgNO_3$ for receiving single-phase material. Multimodal

distribution of pores by the size in Bi_2O_3 pure NPs (figure 3 (d)) after doping by silver changed for unimodal distribution with a maximum about 20-25 nm (figure 3 (d, f)) The improved textural parameters of the NPs Ag-doped Bi_2O_3 indicate the prospect of their use as nanocontainers for drugs.

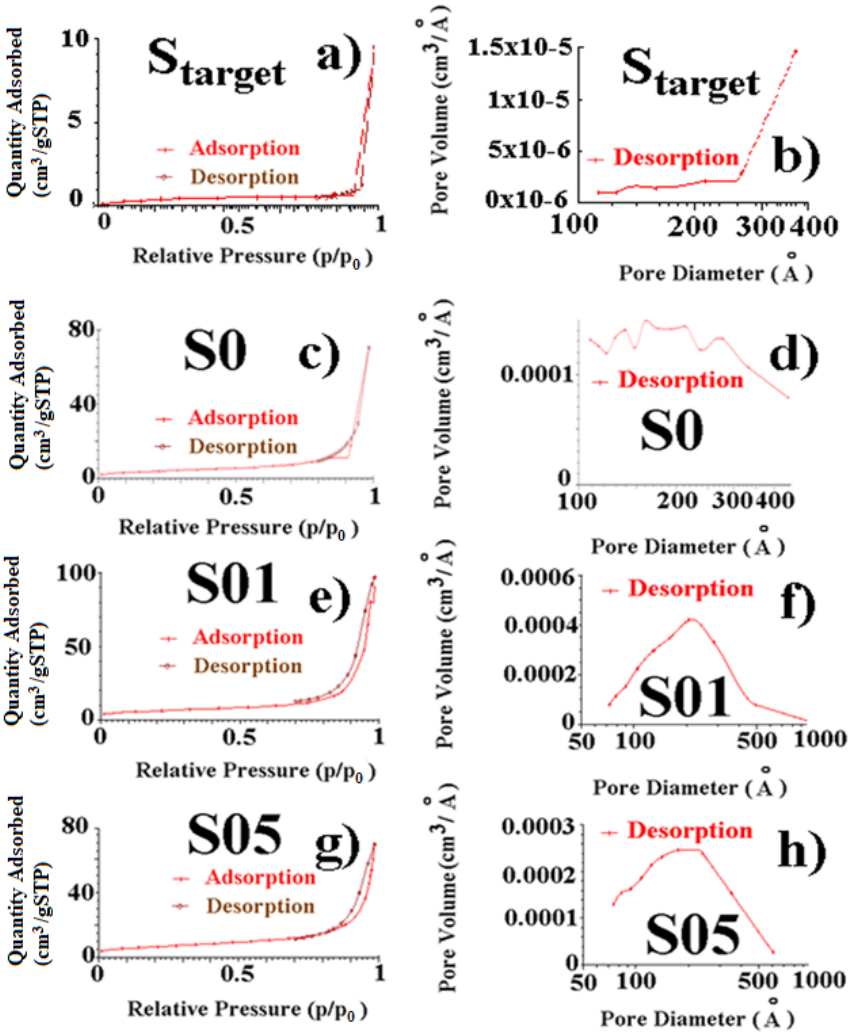

Figure 3. Nitrogen adsorption/desorption isotherm curves (a, c, e, g) and pore size distribution (b, d, f, h) of samples S_{target} and NPs Bi_2O_3 pure, Ag doped Bi_2O_3 (1% $AgNO_3$) ,(5% $AgNO_3$), respectively increase in the specific surface area of silver-containing powders.

3.3. Thermal analysis

We recorded synchronous DSC-TG thermograms and mass spectra of H_2O and CO_2 NPs pure and Ag-doped samples. Analysis of thermograms of sample S0 is given in [6].

Samples S1 and S5 were heated in air at a rate of 10 deg/min in the following mode: primary heating from 40 to 575°C-**I**, then cooling from 575 to 100°C-**II**; secondary heating from 100 to 400°C -**III** and cooling from 400-100°C-**IV**. Thermograms of samples S1 and S5 are similar to each other, therefore the analysis of a sample with 1 wt.% in $AgNO_3$ is for brevity provided. On primary thermogram of heating (**I**) on curve DSC are shown four thermal peaks: the **1**-endothermic peak from evaporation of the adsorbed water in the temperature range 40-220°C, the corresponding synchronous peak was present at H_2O mass spectrum; the **2**-exothermic peak in the temperature range 233-308°C is associated with crystallization of the amorphous fraction of NPs, which was accompanied by simultaneous evaporation of crystallization water from the pores of NPs and the release of gaseous CO_2 as a result of decomposition of bismuth carbonate, the presence of which was very likely. The **3**-exothermic peak is associated with the reaction of decomposition of silver oxide Ag_2O. The **4**-exothermic peak in the temperature range 325-375°C is associated with the phase transition $\beta \rightarrow \alpha$.

The TG curve synchronously, at two sites in the temperature range from 50 to ~ 233°C, showed a decrease in the mass of the sample as a result of several processes in the sample: evaporation of water, removal of carbon during crystallization of the amorphous phase and decomposition of bismuth carbonate (the decomposition of carbonate confirms the second peak on the mass spectrum of H_2O). Starting at 233°C, the TG curve showed continuous weight growth, most likely due to the formation of NPles from silver and bismuth oxides, from metal NPles Bi and Ag, the presence of which in NPs pure Bi_2O_3 was confirmed in early works [6, 8]. The DSC-TG cooling curves after primary heating (**II**), the secondary heating curves (**III**) from 100 to 400°C, and the cooling curve from 400 to 100°C lacked peaks from any phase transformations. This indicates the formation of a dynamic heating stable up to 400°C α-phase in the silver-containing sample due to the doping effect.

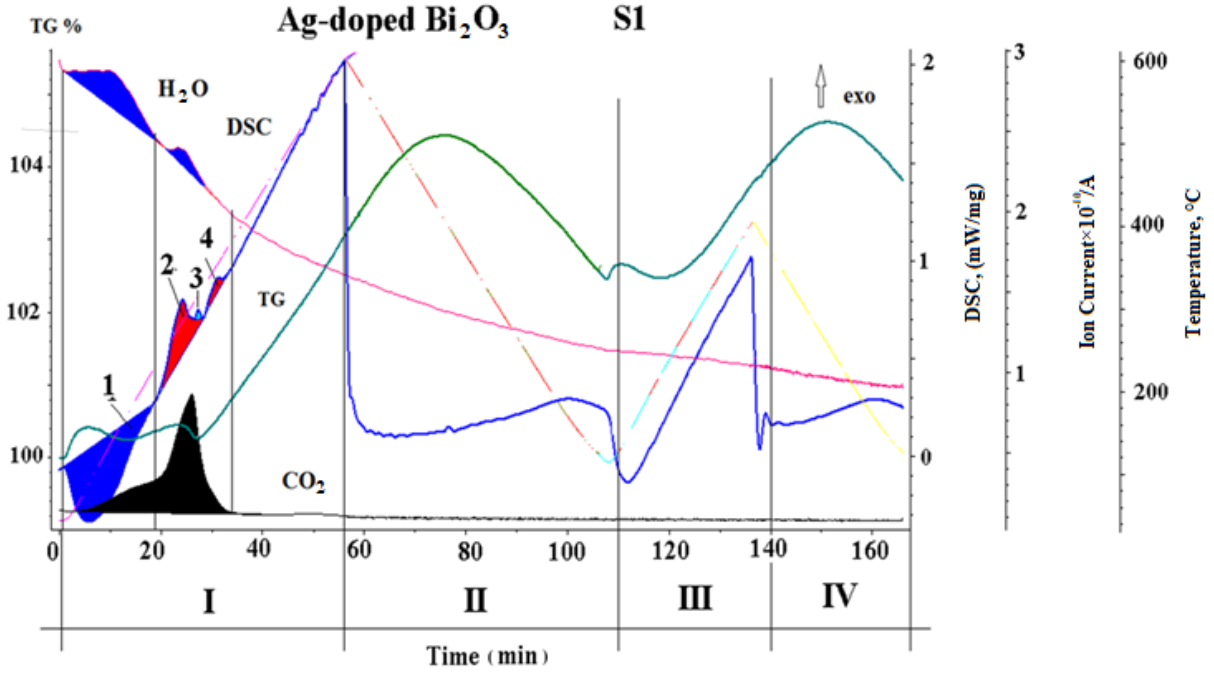

Figure 4. Thermograms DSC-TG heating/cooling in air and mass spectra H_2O and CO_2 of the sample Ag-doped Bi_2O_3 (1% $AgNO_3$). Primary heating/cooling - temperature ranges I and II, secondary heating/cooling - temperature ranges III and IV.

3.4. Magnetic properties of Ag-doped Bi_2O_3 NPs

Figure 5 shows the magnetization curves of the target material (1) and the nanopowder immediately after evaporation (2, 3, 4). The diamagnetic susceptibility of the starting powder Bi_2O_3 was 1.8×10^{-7} cm^3/g, which corresponds to reference data. The ferromagnetic contribution was negligible and did not exceed the measurement errors. Susceptibility of NPs Bi_2O_3 obtained by electron beam evaporation was increased, possibly due to paramagnetic contributions of obscure nature, the presence of which was noted even in single crystals [9]. The ferromagnetic contribution was much more significantly changed - up to 3 memu/g, which significantly exceeds the measurement error. In the work [9], in which were analyzed the properties of massive single crystals Bi_2O_3, was observed no ferromagnetic contribution. Apparently, the appearance of ferromagnetism in bismuth oxide is characteristic only of samples with a large proportion of surface states, such as nanopowders. Such features have been observed for a number of other materials [10], but there is no generally accepted theory that would explain this phenomenon. The addition of silver nitrate from 1 to 5% practically did not change the susceptibility of bismuth oxide nanopowders (curves 3 and 4 to figure 5). A slight decrease in ferromagnetic contribution was observed, the decrease being the same for

samples S1 and S5. Further study of the effect of silver additives at a concentration of less than 1% is required to determine whether this decrease is the result of some other unaccounted for experimental factors.

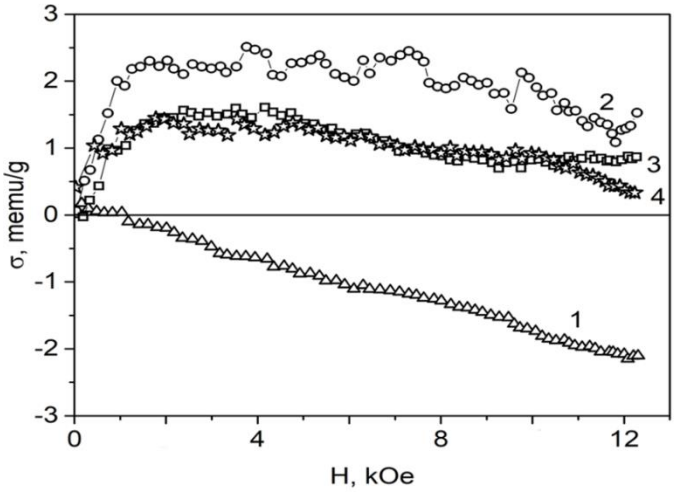

Figure 5. Magnetization curves of target material (1) and nanopowder Bi_2O_3 pure after spraying (2), Ag-doped Bi_2O_3 (1 wt.% $AgNO_3$) (3) and (5 wt.% $AgNO_3$) (4).

4. Conclusion

Using the PEBE method, mesoporous amorphous crystalline NPs Ag-doped Bi_2O_3 were produced in vacuum with little impurity of unidentified silver-containing phase.

The introduction of silver made it possible to stabilize the metastable β-phase in NPs Bi_2O_3, both at room temperature and after annealing the NPs in air up to a temperature of 350°C.

The introduction of silver increased SSA and the pore volume of NPs Bi_2O_3 almost 2 times, reduced the pore diameter by a third, which, in combination with the known antibacterial properties of silver, indicates the prospect of using such NPs in biomedicine.

The insignificant FM response found in pure Bi_2O_3, after doping of Ag samples, was practically unchanged.

Acknowledgments

Authors are grateful to the research scientist of IMF UB RAS, to PhD Gaviko V.S. for XRD NPs. The reported study was funded by RFBR and GACR, project number 20-58-26002.

References

[1] Yukhin Y M and Mikhailov Y I 2001 *Khimiya vismutovykh soedinenii i materialov (Chemistry of Bismuth Compounds and Materials)* (Novosibirsk: Publishing house of the SB RAS) [in Russian]
[2] Gandhi A C, Lai C-Y, Wu K-T, Ramacharyulu P V R K, Koli V B, Cheng C-L, Ke S-C and Wu S Y 2020 *Nanoscale* **12** 24119–37
[3] Kirichenko E A, Kaminsky O I, Zaytsev A V, Makarevich K S and Pyachin S A 2020 *Opt. Spectrosc.* **128** 315–22
[4] Fruth V, Ianculescu A, Berger D, Preda S, Voicu G, Tenea E and Popa M 2006 *J. Eur. Ceram. Soc.* **26** 3011–6
[5] Sokovnin S Yu and Il'ves V G 2012 *Ferroelectrics* **436** 101–7
[6] Ilves V G, Gaviko V S, Malova O A, Murzakaev A M, Sokovnin S Yu, Uimin M A and Zuev M G 2021 *J. Alloy. Compd.* **881** 160514
[7] Gattow G and Schütze D 1964 *Z. Anorg. Allg. Chem.* **328** 44–68
[8] Sokovnin S Y and Il'ves V G 2021 *Tech. Phys. Lett.* **47** 807–10
[9] Nizhankovskii V I, Kharkovskii A I and Orlov V G 2002 *Ferroelectrics* **279** 157–66
[10] Coey J M D 2005 *Solid State Sci.* **7** 660–7